SCANNING ROTATIONAL RAMAN LIDAR AT 355 nm FOR THE MEASUREMENT OF TROPOSPHERIC TEMPERATURE FIELDS

Marcus Radlach, Andreas Behrendt, Sandip Pal, Thorsten Schaberl, Volker Wulfmeyer

Institute of Physics and Meteorology, University of Hohenheim, D-70593 Stuttgart, Germany,
radlach@uni-hohenheim.de, behrendt@uni-hohenheim.de, sandip@uni-hohenheim.de,
schaberl@uni-hohenheim.de, wulfmeye@uni-hohenheim.de

ABSTRACT

A scanning eye-safe lidar system for rotational Raman (RR) temperature profiling at 355 nm was developed at the Institute of Physics and Meteorology (IPM), University of Hohenheim, Germany. A first noontime measurement up to 5 km height is presented here as well as 30 consecutive 60-s profiles covering the upper part of the planetary boundary layer and the lower free troposphere. The receiver is optimized for temperature sensing in the lower troposphere. Performance simulations in order to specify suitable filter parameters were performed and are also discussed. A sequential design of the filter-polychromator provides a very efficient separation of the backscattered light. The filters are used with small angles of incidence and extract RR signals out of the anti-Stokes branch.

1. INTRODUCTION

Temperature is a key parameter of the state of the atmosphere: The temperature gradient – together with humidity – rules atmospheric stability. Thus, high resolution temperature data in both space and time are very beneficial for the study of atmospheric processes. For instance, for investigating the initiation of convection, a key problem of today's numerical weather prediction, continuous 3D temperature fields in the planetary boundary layer and free troposphere are highly desirable [1]. The only remote sensing technique capable of 3D temperature measurements is scanning lidar; such a system, however, has not been realized yet.

The RR technique is a straightforward and rugged lidar technique by which it is possible to measure atmospheric temperature with low statistical errors and high resolution throughout the troposphere and lower stratosphere. Reference [2] demonstrated temperature measurements from 2 km up to 40 km above ground. Most systems are using a wavelength of 532 nm. So far only one publication exists which presented RR measurements in the UV [3]. The main reason for this preference was the poor performance of narrow-band interference filters and gratings in the UV that prevailed a long time. New techniques in manufacturing the filters are now allowing better optical performance, namely, transmission values, that exceed 50%, and high out-of-band blocking.

The larger molecular backscatter coefficient at lower wavelengths is advantageous for the use of 355 nm in the troposphere. In addition, compared to the conventionally used 532 nm, better detector efficiencies and a lower solar background in case of daytime operations are very beneficial for RR lidar in the UV. Thus, we can expect that the better performance of narrow-band interference filters in the UV which can be realized today leads to better system performance throughout the troposphere than for comparable systems at 532 nm [4].

We have developed a lidar receiver for RR temperature profiling at 355 nm. A sequentially mounting of the filters leads to high efficiency in extracting the signals [5]. By use of a scanner it is possible for the first time to perform 3D scans of temperature fields in the atmosphere.

2. SYSTEM SETUP

The scanning RR lidar of IPM is a mobile system, which is mounted into a container that is fixed onto a truck. The existing eye-safe scanning aerosol lidar at 355 nm [6] was extended by the integration of two RR channels. The third-harmonic radiation of an unseeded flash-lamp-pumped Nd:YAG laser from Spectra-Physics, model GCR5-30 is used, with a pulse repetition rate of 30 Hz and pulse energy of about 300 mJ. The beam at 355 nm is expanded to a diameter of 65 mm. A roof-mounted scanner, manufactured by the National Center for Atmospheric Research (NCAR) in Boulder, is pointing the beam in any direction. The backscattered light from the atmosphere is directed via two scanner mirrors to a telescope with a primary-mirror diameter of 40 cm. After passing the field stop plane and collimation, the light is coupled into a fiber and is guided to the polychromator.

The data acquisition system is a 3-channel transient recorder of Licel GmbH, Germany. The data of each lidar channel are recorded in two modules; in analog and photon-counting mode with 3.75 m resolution up to heights of 15 km in the first module and in photon-counting mode with 36 m resolution up to 73 km in the second module.

The setup of the polychromator for extracting the lidar signals out of the light backscattered from the atmosphere is shown in Fig. 1. Inside the polychromator, a lens collimates the light exciting the fiber. A chain of

narrow-band interference filters aligned with small angles of incidence (AOI) extracts three signals from the backscattered light: the elastic signal and two RR signals of opposite temperature dependence within the anti-Stokes branch. The intensities of the lines within the pure RR bands of atmospheric nitrogen and oxygen depend differently on temperature. The intensities of lines close to the incident laser line decrease with rising temperature, while the intensities of lines with large wavelength differences increase. This feature is a result of the population of rotational energy levels, which is described by a Maxwell-Boltzmann distribution. With the ratio of two RR lidar signals of opposite temperature dependence one has a quantity that is independent of atmospheric transmission and range and provides after a calibration of the system directly the atmospheric temperature [7].

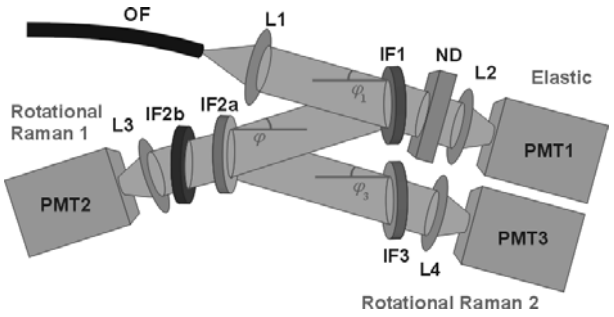

Fig. 1: Scheme of the rotational Raman lidar polychromator, which is coupled by a fiber to the receiving telescope. OF, optical fiber; L1 – L4, lenses; IF1 – IF3 interference filters; ND, optional neutral-density filter; PMT1-PMT3, photomultiplier tubes.

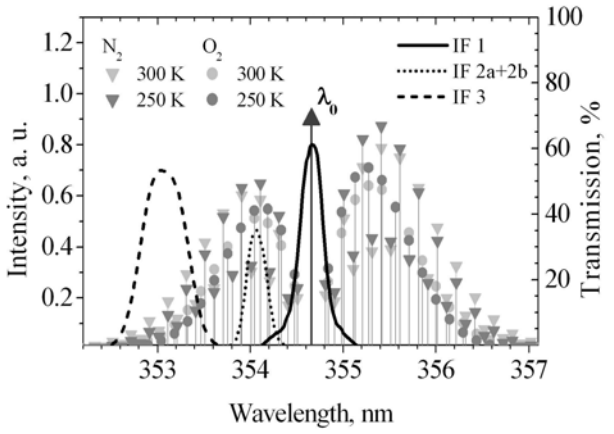

Fig. 2: Transmission curves of the narrow-band interference filters used in the rotational Raman lidar polychromator together with the rotational Raman spectrum for temperatures of T_1 = 300 K and T_2 = 250 K. λ_0 labels the wavelength of the laser at 354.66 nm.

The cascade structure of the polychromator illustrated in Fig. 1 has some important advantages to other set-ups [5]. First, the central wavelengths (CWL) can be tuned by increasing the tilting angle φ of the filters. Second, a very high suppression of the elastically scattered light in the RR channels is achieved. Because the transmission band of IF2 is very close to the laser wavelength we need two filters for the first RR channel. Third, we get very high efficiency when separating the light in the receiver. The transmission curves of the narrow-band interference filters manufactured by Barr Associates are shown in Fig. 2. The filter parameters are summarized in Tab. 1.

Table 1: Parameters of the narrow-band interference filters of the rotational Raman lidar polychromator.

	IF 1	IF 2a	IF 2b	IF 3
AOI, deg	5.7	6.5	6.5	6.0
CWL, nm	354.66	354.05	354.05	353.07
FWHM, nm	0.29	0.32	0.33	0.52
Peak Transmission	0.62	0.53	0.65	0.52
Reflectivity at 354.66 nm	< 0.1			
Transmission at 354.66 nm		$< 10^{-3}$	$< 10^{-3}$	$< 10^{-6}$

3. FILTER CALCULATIONS

We have performed detailed performance simulations in order to specify the parameters of the filters that are used to extract the pure RR signals out of the atmospheric backscatter. For this, we simulated the expected statistical temperature uncertainties if the filters are set to different CWLs and filter widths (full width at half maximum, FWHM) at different atmospheric temperatures. Additionally we added a background signal, which was scaled to the filters FWHM. The 1-σ statistical uncertainty of temperature measurements with the RR technique can be calculated by [8]:

$$\Delta T = \frac{\partial T}{\partial Q}\Delta Q \approx \frac{(T_1 - T_2)}{(Q_1 - Q_2)} Q \sqrt{\frac{P_{RR1} + 2P_{B1}}{P_{RR1}^{\,2}} + \frac{P_{RR2} + 2P_{B2}}{P_{RR2}^{\,2}}} \quad (1)$$

Q is the ratio of the two temperature-dependent RR signals P_{RR1} and P_{RR2}. P_{B1} and P_{B2} are the background signals. We calculated the errors for different pairs of temperature (T_1, T_2) ranging from 270 to 220 K and 275 to 225 K, respectively, with the ratios Q_1 and Q_2. The uncertainties are becoming minimum for a certain combination of high temperature sensitivity and large signal intensities.

We found that a setup of broader filters with different FWHM is the better choice due to the higher intensities of the extracted signals and the higher transmission

values than narrower filters. If we assume equal transmission values for a pair of filters with $\Delta\lambda_{FWHM1} = \Delta\lambda_{FWHM2} = 0.05$ nm and a set of broader filters with $\Delta\lambda_{FWHM1} = 0.3$ nm and $\Delta\lambda_{FWHM2} = 0.5$ nm (the widths of our filters), still the setup of the broader filters shows much lower temperature errors in case of no background, whereas the errors are almost equal in case of an additional background signal regardless of the intensity of the background.

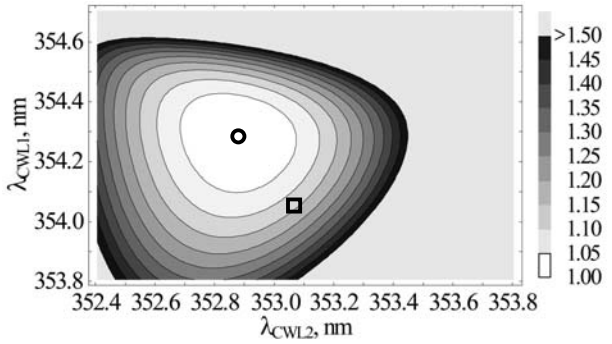

Fig. 3: Calculated statistical temperature uncertainty ΔT versus filter CWLs λ_{CWL1} and λ_{CWL2} for our filters (Fig. 2), (T_1, T_2) = (270 K, 275 K). The exciting wavelength is 354.66 nm. Calculation step width was 0.01 nm. Values for ΔT (scale on the right) are plotted relatively to the minimum at $\lambda_{CWL1} = 354.28$ nm and $\lambda_{CWL2} = 352.88$ nm (black circle). The black square marks our filter setup.

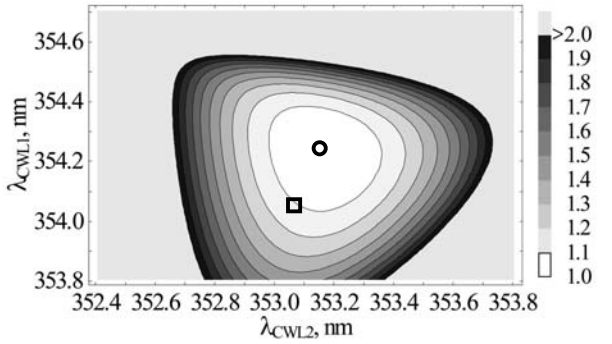

Fig. 4: Same as Fig. 3 but with a background signal of the same intensity as the strongest rotational Raman line in the anti-Stokes branch added to the signals. The minimum is at $\lambda_{CWL1} = 354.23$ nm and $\lambda_{CWL2} = 353.16$ nm (black circle).

Calculations for the filters from Tab. 1 are shown in Fig. 3 without and Fig. 4 with a background signal and (T_1, T_2) = (270 K, 275 K). For this simulation we took the wavelength of our laser, 354.66 nm, into account. From Fig. 3 and Fig. 4 it is obvious that there is only a shift of the optimum of λ_{CWL2} towards a longer wavelength in case of an additional background signal. This shift is barely increasing for even much larger background values. Also lower temperatures down to 220 K result only in a shift of the optimum λ_{CWL2} of about 0.15 nm towards longer wavelengths. In addition, Fig. 3 and 4 show that we easily can improve our measurement sensitivity by changing λ_{CWL2}. This tuning of IF3 does not require any further adjustments of the other channels.

4. MEASUREMENT EXAMPLE

A daytime measurement at about noontime was performed on 27 March 2006. The calibration of the ratio of the measured lidar signals is shown in Fig. 5. The resolution of the raw data is 60 m and 60 s. To calibrate the lidar, the signals were summarized over the last 20 minutes of the measurement period to minimize statistical uncertainties. The data beyond low clouds present in about 1.6 km height in the first 10 minutes have been excluded. Only the background corrected raw data of the analog signals up to 5 km height are used. Calibration constants were determined by a single line approach (dashed line, Fig. 5), which results in $A = -567.7$ K and $B = 1.73$. The approximation that considers the extraction of multiple lines (doted line, Fig. 5) [4], however, leads not to a more accurate calibration.

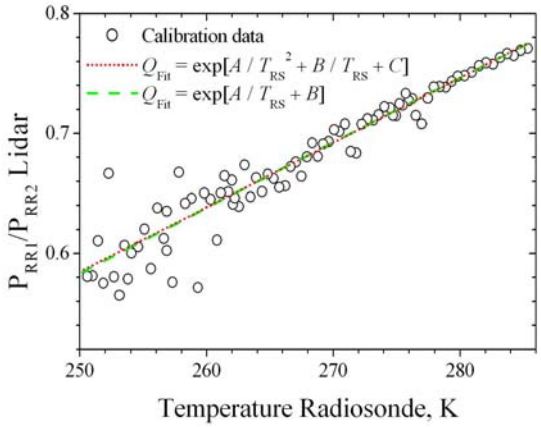

Fig. 5: Ratio of the lidar signals P_{RR1} and P_{RR2} plotted versus the temperature of a nearby radiosonde and calibration curves.

Fig. 6 shows the calibrated temperature profile of the lidar and a nearby radiosonde (13 km distance), which was launched close in time. At heights below 500 m the profile is distorted due to insufficient overlap in the near range. After applying a gliding average of 120 m below and 600 m above 1.5 km, ΔT remains below ± 1 K up to a height of 3 km. The statistical uncertainty of the temperature measurement was derived with an algorithm

that matches the analog signals to the photon-counting signals of the same resolution. The adjusted analog signals were used to calculate ΔT with Eq. 1. A time-height cross section of the temperature with 60 s profiles is shown in Fig. 7.

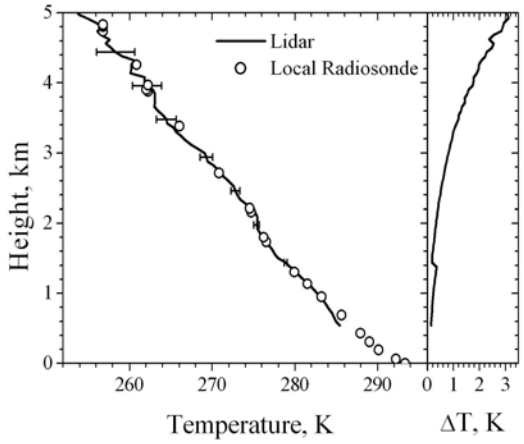

Fig. 6: Lidar temperature profile (straight line) and radiosonde (circles) from 12 UTC on 27 March 2006 (left). The lidar profile is smoothed with a gliding average of 120 m below 1.5 km height and with 600 m above. Error bars and the profile in the right panel show statistical temperature uncertainty.

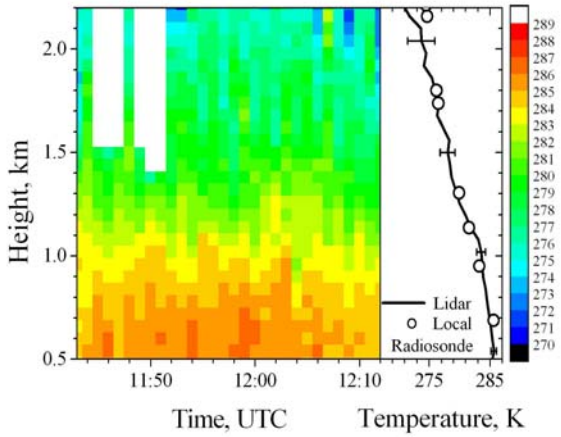

Fig. 7: Time-height cross section of 60-s temperature profiles between 11:43-12:13 UTC on 27 March 2006 (left) and lidar profile with error bars (straight line) from 11:56 UTC and radiosonde (circles) from 12 UTC (right). Lidar signals were smoothed with a gliding average of 240 m. Error bars show the statistical temperature uncertainty. The temperature scale is plotted on the right.

The profiles were smoothed with a gliding average of 240 m. The profile of 11:56 UTC is shown on the right side. The statistical measurement uncertainty ΔT is not exceeding 1 K up to 1 km height and stays below 3 K up to 2 km. The sharp decrease in temperature seen in the plot between 0.5 km and 2 km is close to the dry adiabatic laps rate. This condition was favorable for strong thunderstorms that day, which developed later in the afternoon.

5. SUMMARY & OUTLOOK

The first data of our new rotational Raman lidar demonstrate the capability for daytime temperature measurements even at noontime with $\Delta T < 1$ K up to 1 km and $\Delta T < 3$ K up to 2 km for a temporal resolution of 60 s and a vertical resolution of 240 m. Besides vertical temperature profiling we are able to measure temperature in any other pointing directions, too. These measurements are planned for the near future and will enable observing the 3D structure of the temperature field in the planetary boundary layer and the lower troposphere for the first time.

Also the particle extinction and backscatter coefficient are parameters that are measured with the RR technique [8]. Our scanning rotational Raman lidar will be employed in July 2006 during the measurement campaign PRINCE (PRediction, Identification and trackiNg of Convective cElls) in the Northern Black Forrest.

We also plan to install a high-power diode-pumped Nd:YAG laser, which will be seeded, and a interferometer for further improvement of the daytime temperature measurement performance [9]. With this setup the lidar system will be operated during the COPS campaign (Convective and Orographically-induced Precipitation Study) in summer 2007 [1].

ACKNOWLEDGMENT

The development of the RR lidar was performed within the virtual institute COSI^{TRACKS} (COnvective Storms virtual Institute - a contribution to TRACKS; Transport and Chemical Conversion in Convective Systems).

6. REFERENCES

1. Behrendt, A., et al., this conference, 2006.
2. Behrendt, A., et al., *Appl. Opt.* **43**, 14, 2930-2939, 2004.
3. Di Girolamo, P., et al., *Geophys. Res. Lett.* **31**, L01106, doi:10.1029/2003GLO18342, 2004.
4. Behrendt, A., Temperature Measurements with Lidar, In: C. Weitkamp (Ed.) *Lidar*, Springer-Verlag, New York, 2005.
5. Behrendt, A., and Reichardt, J., *Appl. Opt.* **39**, 9, 1372-1378, 2000.
6. Pal, S., et al., this conference, 2006.
7. Cooney, J., *J. Appl. Meteorol.* **11**, 108-112, 1972
8. Behrendt, A., *Appl. Opt.* **41**, 36, 7657-7666, 2002.
9. Arshinov, Y., et al., *Appl, Opt.* **44**, 17, 3539-3603, 2005.